Published in final edited form as:
Synapse. 2013 November ; 67(11): 757–772. doi:10.1002/syn.21683.

Stress differentially alters mu opioid receptor density and trafficking in parvalbumin-containing interneurons in the female and male rat hippocampus

Teresa A. Milner[1,3], **Suzanne R. Burstein**[1], **Gina F. Marrone**[1], **Sana Khalid**[1], **Andreina D. Gonzalez**[1], **Tanya J. Williams**[1,2], **Kathryn C. Schierberl**[1], **Annelyn Torres-Reverón**[4], **Keith L. Gonzales**[1], **Bruce S. McEwen**[3], and **Elizabeth M. Waters**[3]

[1]Brain and Mind Research Institute, Weill Cornell Medical College, 407 East 61st Street, New York, NY 10065

[2]Weill Cornell/Rockefeller/Sloan-Kettering Tri-Institutional MD-PhD Program, New York, NY 10065

[3]Harold and Margaret Milliken Hatch Laboratory of Neuroendocrinology, The Rockefeller University, 1230 York Avenue, New York, NY 10065

[4]Departments of Physiology and Pharmacology / Psychology, Ponce School of Medicine and Health Sciences, Ponce, Puerto Rico

Abstract

Stress differentially affects hippocampal dependent learning relevant to addiction and morphology in male and female rats. Mu opioid receptors (MORs), which are located in parvalbumin (PARV)-containing GABAergic interneurons and are trafficked in response to changes in the hormonal environment, play a critical role in promoting principal cell excitability and long-term potentiation. Here, we compared the effects of acute and chronic immobilization stress (AIS and CIS) on MOR trafficking in PARV-containing neurons in the hilus of the dentate gyrus in female and male rats using dual label immuno-electron microscopy. Following AIS, the density of MOR silver-intensified gold particles (SIGs) in the cytoplasm of PARV-labeled dendrites was significantly reduced in females (estrus stage). Conversely, AIS significantly increased the proportion of cytoplasmic MOR SIGs in PARV-labeled dendrites in male rats. CIS significantly reduced the number of PARV-labeled neurons in the dentate hilus of males but not females. However, MOR/PARV-labeled dendrites and terminals were significantly smaller in CIS females, but not males, compared to controls. Following CIS, the density of cytoplasmic MOR SIGs increased in PARV-labeled dendrites and terminals in females. Moreover, the proportion of near-plasmalemmal MOR SIGs relative to total decreased in large PARV-labeled dendrites in females. After CIS, no changes in the density or trafficking of MOR SIGs were seen in PARV-labeled dendrites or terminals in males. These data show that AIS and CIS differentially affect available MOR pools in PARV-containing interneurons in female and male rats. Furthermore, they suggest that CIS could affect principal cell excitability in a manner that maintains learning processes in females but not males.

Keywords

opioids; sex differences; estrogens; chronic stress; acute stress

*Address correspondence to: Dr. Teresa A. Milner, Brain and Mind Research Institute, Weill Cornell Medical College, 407 East 61st Street, RM 307, New York, NY 10065, Phone: (646) 962-8274, FAX: (646) 962-0535, tmilner@med.cornell.edu.

Introduction

In humans and animals, areas involved in learning and memory, including the hippocampus, are strongly activated during craving induced by drug-associated cues (Kilts et al., 2001;Risinger and Oakes, 1995;Volkow et al., 2006). Contextual cue induced reinstatement to drug use critically depends on hippocampal output (Atkins et al., 2008;Crombag et al., 2008), relayed directly from the subiculum or indirectly from the CA2/CA3a region to the mesolimbic reward system (Luo et al., 2011;Vorel et al., 2001). The hippocampus is involved in reinstatement of abuse of heroin as well as other pharmacological classes of drugs (Bossert et al., 2007;Rogers et al., 2008). Moreover, the hippocampus, particularly the endogenous opioid system, has been implicated in addiction to opiates, i.e., morphine, heroin and oxycodone, and other drugs (Gerrits et al., 2003;Hyman and Malenka, 2001;Leshner, 2002;Nestler, 2001).

Drug addiction, particularly relapse, is often provoked by stress [reviewed by (Bruchas et al., 2008;Shalev et al., 2000)]. Although stress has powerful influences on addictive processes in both males and females (Koob, 2008), females have a heightened sensitivity to stress (Becker et al., 2007) that may contribute to their accelerated course of addiction (Elman et al., 2001;Hu et al., 2004;Lynch et al., 2000;Robbins et al., 1999). In addition, the rate and triggers of drug abuse relapse differ between men and women (Fiorentine et al., 1997;Weiss et al., 1997).

Sex differences in response to acute and chronic stress have been reported in hippocampal learning and circuitry (Bowman et al., 2003;Conrad et al., 2003;Luine et al., 2007). In males, chronic stress impairs cognitive performance on spatial memory tasks as well as on non-spatial recognition memory tasks and decreases long-term potentiation (LTP) [for reviews see (Luine et al., 2007;McEwen and Milner, 2007)]. Additionally, chronic stress in males results in the debranching and atrophy of the apical dendrites on CA3 pyramidal cells (McEwen, 1999;Vyas et al., 2002), increases the packing density of small synaptic vesicles near the active zones of mossy fiber terminals (Magarinos et al., 1997), decreases the number of parvalbumin (PARV) -containing inhibitory interneurons (Czeh et al., 2005;Hu et al., 2010) and suppresses adult neurogenesis (Pham et al., 2003). Conversely, chronic stress in females does not affect or slightly increases performance on the same memory tasks (Conrad et al., 2003;Kitraki et al., 2004;Luine et al., 2007) and does not result in severe atrophy of CA3 pyramidal cell apical dendrites (Galea et al., 1997; McLaughlin et al., 2010).

Hippocampal regions that are vulnerable to the sexually dimorphic effects of stress extensively overlap with the endogenous opioid system. The mossy fiber pathway is rich in the opioid peptides, enkephalin and dynorphin, as well as the mu opioid receptor (MOR) 1D slice variant [reviewed in (Drake et al., 2007)]. Additionally, MOR-1As (hereafter referred to as MORs) are expressed prominently in PARV-containing interneurons whereas delta opioid receptors (DORs) are expressed prominently in somatostatin, neuropeptide Y and/or corticotropin releasing factor (CRF) interneurons and in pyramidal cells (Drake et al., 2007;Williams and Milner, 2011). Activation of MORs and DORs, either by endogenous opioids or exogenous agonists such as morphine can enhance pyramidal cell excitability via disinhibition and can facilitate LTP (reviewed by (Simmons and Chavkin, 1996)).

Emerging evidence indicates that gonadal steroids and stress can both impact the hippocampal opioid system. Ovarian hormone levels can alter the levels of enkephalins and dynorphins in the mossy fiber pathway (Torres-Reveron et al., 2008;Torres-Reveron et al., 2009a) and trafficking of MORs in PARV-containing interneurons (Torres-Reveron et al., 2009b). Moreover, the proportion of DOR interneurons containing CRF as well as the trafficking of DORs in pyramidal cells varies with sex and ovarian hormone status

(Williams et al., 2011b;Williams and Milner, 2011). Following exposure to stress, opioid peptides are released in the hippocampus (McLaughlin et al., 2003) where they can bind extrasynaptically to nearby MORs (Drake et al., 2002). Recently, we have shown sex-differences in the activation of both hippocampal MORs and DORs following acute stress (Burstein et al., 2013;Gonzales et al., 2011). However, whether stress also affects the trafficking or density of opioid receptors in hippocampal neurons is unknown.

Thus, the present study sought to determine if trafficking and/or density of MORs is altered in the hippocampus following stress, and if so, does this differ in males and cycling females. For this, dual labeling electron microscopic immunocytochemistry examined the distribution of MORs in PARV-labeled interneurons in the hilus of the dentate gyrus in males and cycling females after acute and chronic immobilization stress (AIS and CIS, respectively).

Materials & Methods

Animals

All procedures were approved by the Rockefeller University and Weill Cornell Medical College Institutional Animal Care and Use Committees and were in accordance with the 2011 Eighth edition of the National Institutes of Health guidelines for the Care and Use of Laboratory Animals. Adult male and female Sprague Dawley rats (~60d old, N = 84) from Charles River Laboratories (Wilmington, MA) were housed 3–4 animals per cage with 12:12 light/dark cycles. Rats could access food and water *ad libitum*.

Estrous cycle determination—Only female rats that showed two consecutive, regular 4–5 day estrous cycles prior to initiation of the stressor were used. Estrous cycle stage was determined using vaginal smear cytology (Turner and Bagnara, 1971) daily between 9:00 and 10:00 AM, following one week of acclimation following arrival. To control for the effects of handling, male rats were removed from their cages daily to perform mock estrous cycling. Uterine weight and plasma serum estradiol levels via radioimmunoassay (Torres-Reveron et al., 2008) were measured to confirm estrous cycle stage. Diestrus 2 rats rather than metestrus (diestrus I) were chosen to ensure that rats were completely out of the estrus stage.

Acute Immobilization Stress—Rats were transported from their home room into a procedure room, and AIS was performed as previously described (Lucas et al., 2007;Shansky et al., 2010) between 9:00 AM and 1:00 PM. Rats were placed in plastic cone shaped polyethylene bags with a Kotex mini-pad underneath them to collect urine and small hole at the apex of the cone. Animals were placed with their nose at the hole, sealed with tape in the bag, and left undisturbed on the countertop for 30 minutes. Immediately after, rats were anesthetized in a neighboring procedure room and fixed via perfusion (see below). Control rats were left in the home room and anesthetized prior to transfer to the procedure room for perfusion.

Chronic immobilization stress—Rats were subjected to AIS as described above for 10 consecutive days. Both CIS and control rats were pair housed in cages. During the stress paradigm, CIS rats were housed in a separate room. Rats were killed 1 day after the last stress period.

Immunocytochemistry

Antibodies—A rabbit polyclonal antibody against MOR1A was purchased originally from Neuromics (Minneapolis, MN; now incorporated with Chemicon at Millipore). This antibody recognizes residues 384–398 from the carboxy terminus of MOR1 and does not

recognize the splice variant MOR-1B–E or the cloned DOR (Abbadie et al., 2000;Arvidsson et al., 1995). Specificity of the antibody has been demonstrated previously by western blotting, pre-adsorption and omission controls in brain tissues (Arvidsson et al., 1995;Drake and Milner, 1999). A mouse monoclonal PARV antibody was purchased from Sigma (St. Louis, MO). This antibody has been previously characterized by radioimmunoassay, immunoblots and the ability to recognize PARV in brain tissue (Celio, 1990).

Section preparation—Rats were deeply anesthetized with sodium pentobarbital (150mg/kg, I.P.) and perfused sequentially through the ascending aorta with: 1) 10–15ml 0.9% saline containing 2% heparin; 2) 50 ml of 3.75 % acrolein and 2% paraformaldehyde in 0.1M phosphate buffer (PB; pH7.4); and 3) 200ml of 2% paraformaldehyde in PB. After perfusion, brains were cut into 5 mm coronal blocks, post-fixed in 2% paraformaldehyde in PB for 30 min, and then transferred into PB. Coronal sections (40μm thick) through the hippocampus were cut on a vibrating microtome (Leica Microsystems, Buffalo Grove, IL) into PB. Sections were stored in cryoprotectant solution (30% sucrose and 30% ethylene glycol in PB) at −20 °C. Prior to immunocytochemistry, sections were rinsed in PB, coded with hole-punches and pooled into containers to ensure identical processing (Pierce et al., 1999). (Note: Females and males from AIS and CIS groups were processed in separate sets. Thus, the density of MOR labeling from females and males could not be directly compared.) Sections were incubated in sodium borohydride (1% in PB) for 30 minutes and rinsed in PB.

Light microscopic immunocytochemistry—To examine changes in the number of PARV-labeled cells between different experimental groups, sections were processed as previously described (Torres-Reveron et al., 2009b). Briefly, sections were transferred to 0.1M Tris-buffered saline (TS; pH7.6) and then blocked in 0.5% bovine serum albumin (BSA) in TS for 30 minutes in PB. Sections were placed in mouse PARV antibody (1:3000) for 24 hours at room temperature, and then 24 hrs at 4°C. Sections then were processed in a 1:400 dilution of biotinylated horse-anti mouse immunoglobulin (IgG; Vector Laboratories, Burlingame, CA) for 30 min followed by a 1:100 dilution of avidin-biotin complex (ABC; Vectastain elite kit, Vector Laboratories) for 30 min. All incubations were separated by washes of TS. Sections were reacted in 2,2-diaminobenzidine (DAB; Sigma-Aldrich, St. Louis, MO) and 3% H_20_2 in TS for 6 min and rinsed in TS followed by PB. Sections were mounted on gelatin-coated slides, dehydrated and coverslipped from xylene with DPX mounting media (Sigma-Aldrich).

To dually label MOR and PARV, single sections were incubated in the MOR antibody (1:1000 dilution) for 2 days at 4°C and then the PARV antibody (1:1500) was added to the diluent for an additional day. Sections were rinsed in TS and incubate sequentially in Alexa Fluor 488 goat anti-rabbit IgG and Cy5 goat anti-mouse IgG (both at 1:400 dilution; Invitrogen-Molecular Probes, Carlsbad CA) for 1 hr each. Sections were mounted on gelatin-coated slides, air-dried and coverslipped with slowFade Gold antifade reagent (Invitrogen-Molecular Probes, Grand Island, NY). Immunofluorescent photographs from the dentate gyrus were acquired using a Leica (Nussloch, Germany) confocal microscope. Z-stack analysis was employed to verify dually labeled neurons.

Electron microscopy—Sections were dually labeled for MOR and PARV as described previously (Torres-Reveron et al., 2009b). In brief, sections were incubated in the MOR antibody (1:1000 dilution) in 0.1% BSA and TS for 4 days at 4°C. Two days prior to processing, PARV antibody (1:3000 final dilution) was added to the vial containing the MOR antibody. Sections then were processed for peroxidase labeling for PARV as described for light microscopy. Next, sections were rinsed in TS and incubated in goat anti-rabbit IgG conjugated to 1 nm gold particles [1:50, Electron Microscopy Sciences (EMS), Fort Washington, PA] in 0.01% gelatin and 0.08% BSA in 0.01M phosphate-buffered saline

(PBS; pH 7.4) at 4°C overnight. Sections were rinsed in PBS, post-fixed in 2% glutaraldehyde in PBS for 10 minutes, and rinsed in PBS followed by 0.2 M sodium citrate buffer (pH 7.4). The conjugated gold particles were enhanced by reaction in a silver solution (RPN491 Silver Enhance kit, GE Healthcare, Waukeska, WI) for 5 minutes.

Sections were fixed in 2% osmium textroxide for 1 hour followed by PB rinses and dehydration in increasing concentrations of ethanol and propylene oxide before being embedded in Embed 812 (EMS) (Milner et al., 2011). Ultrathin sections (70–72 nm thick) were cut from the hilus of the dentate gyrus on a Leica UCT ultratome and collected on 400 mesh thin-bar copper grids (EMS). The grids were counterstained with uranyl acetate and Reynolds lead citrate.

Fluoro-Jade staining

To assess if cells in the dentate hilus were degenerating after CIS, hippocampal sections from males and estrus females were processed for Fluoro-Jade staining (Schmued et al., 1997). Sections from male rats subjected to kainic acid-induced seizures (Skyers et al., 2003) were used as positive control. Briefly, sections were treated in sodium borohydride as described above, mounted on Superfrost slides (Esco, Erie Scientific Co., NH), and incubated in Fluoro-Jade ® B (Millipore) according to manufacturer's instructions. Sections were mounted with DPX and viewed on a Nikon H550L microscope equipped with a Nikon Eclipse 90i camera.

Analysis

An experimenter who was blind to treatment group performed all analyses.

Light microscopy—Sections from the dorsal hippocampus (−3.6 to −4.0 mm from Bregma; Swanson 2000) were chosen for analysis. Using the granule cell layer as a border, all labeled cells (PARV or Fluorojade) with a distinguishable nucleus were counted in the dorsal hilus excluding those cells in the CA3 pyramidal cell layer border. Data was analyzed using an unpaired Student's t-test ($p < 0.05$) using Excel for Mac 2011.

Electron microscopy (EM)—Sections from the hilus of the dentate gyrus were examined on a Tecnai transmission electron microscope. Profiles were identified and categorized using standardized morphological characteristics (Peters et al., 1991). Dendritic profiles contained regular microtubular arrays and were usually postsynaptic to axon terminal profiles. Axon terminal profiles had numerous small synaptic vesicles and had a cross-sectional diameter greater than 0.2 μm.

Single ultra-thin sections taken from the surface of sections from the dentate hilus were examined from 3 rats from each experimental condition. Immunoperoxidase labeling for PARV was distinguished as an electron-dense reaction product precipitate. Silver-intensified immunogold (SIG) labeling for MOR appeared as black electron-dense particles. To avoid false negative labeling of smaller profiles, profiles were considered as dual-labeled if they contained electron-dense reaction product and at least one gold particle. Criteria for field selection included good morphological preservation, the presence of immunolabeling in the field, and proximity to the plastic-tissue interface (i.e., the surface of the tissue) to avoid problems due to differences in antibody penetration (Milner et al., 2011). Micrographs containing dual labeled profiles were collected in random fields of the hilus. Tissue collection from each block was terminated when 50 dual labeled dendritic profiles and at least 30 dual labeled terminals were counted.

The subcellular distribution and density of MOR SIG particles in PARV-labeled dendrites and terminals was determined as previously described (Torres-Reveron et al., 2009b). To maintain consistency between this and our previous studies, dendrites were divided into two size categories: small (< 1μm in diameter) and large (> 1 μm in diameter). In general, small and large dendrites correspond to distal and proximal portions of the dendritic tree, respectively. For the analysis, MOR SIG particle localization was recorded as either cytoplasmic, plasmalemmal or "near plasma membrane" (i.e., particles within 50 nM, but not touching, the plasma membrane). SIG particles on the plasma membrane reflect receptors available for ligand binding (Boudin et al., 1998). Several ratios were calculated based on these designations: 1) plasma membrane SIG particles to total number of SIG particles (PL:Total); 2) near plasma membrane SIG particles to total number of SIG particles (Near:Total); and 3) cytoplasmic SIG particles to total number of SIG particles (CY:Total). Morphological parameters that were used as indirect measures of dendrite size, including surface area (perimeter), cross-sectional area, and average diameter, were measured using Microcomputer Imaging Device software (MCID, Imaging Research Inc, Ontario, Canada). These measurements were used to determine the number of plasmalemmal MOR SIG particles in a profile / profile perimeter (PL:μm) and the number of cytoplasmic MOR SIG particles in a profile / profile cross-sectional area (CY:μm^2). Data was analyzed using an unpaired Student's t-test ($p < 0.05$) performed using JMP10 (SAS Institute, Inc.). Datasets were tested for normality.

Figure preparation—Images were cropped in Adobe Photoshop 9.0 prior to importing into PowerPoint 2010 on an iMac, where final adjustments to brightness, contrast and size were made. These changes did not alter the original content of the raw image. Graphs were generated in Prism.

Results

Estrous cycle effects on MOR trafficking in PARV-labeled dendrites

Our previous study (Torres-Reveron et al., 2009b) showed that the number of MOR SIG particles on the plasmalemma of PARV-labeled dendrites in the dentate hilus was greater in proestrus compared to diestrus rats. In the present study, although we found that the CIS group had normal estrous cycles, we wanted to compare estrus rats as this stage has mid-estradiol levels. As this stage had not been studied previously, we first compared the trafficking of MORs in PARV-labeled dendrites from proestrus rats to estrus rats in the dentate hilus of control rats from the AIS group.

By light microscopy, numerous MOR-labeled cells containing PARV-immunoreactivity (ir) were detected in the subgranular zone of the dentate hilus of both proestrus and estrus female rats (Fig. 1A, B). In agreement with our earlier studies (Drake and Milner, 2006;Torres-Reveron et al., 2009b), the distribution of MOR-PARV cells was identical to that seen in males. By electron microscopy, MOR SIG particles were easily identifiable within PARV-labeled dendrites (Fig. 1C). MOR SIG particles were in the cytoplasm as well as on or near the plasmalemma of PARV-containing dendrites. Consistent with the morphology of interneurons (Ribak et al., 1990), MOR-PARV-labeled dendrites were contacted by numerous terminals, many of which formed asymmetric synapses. MOR SIG particles also were seen on the plasmalemma and in the cytoplasm of PARV-labeled terminals (for example, see Fig. 7A).

In control rats, the distribution of MOR SIG particles in PARV-labeled dendrites from proestrus and estrus rats was similar, but there were some differences. Specifically, proestrus females displayed significantly increased ($p<0.05$) total number of MOR SIG particles in PARV-labeled dendrites in comparison to estrus females (Fig. 1D). Within MOR-PARV-

labeled small dendrites, proestrus females had fewer ($p<0.05$) MOR SIG particles on the plasmalemma and increased cytoplasmic density ($p<0.01$) of MOR-SIG particles in comparison to estrus females (Fig. 1E). Proestrus females also showed an increased ratio ($p<0.05$) of cytoplasmic:total MOR SIG particles in PARV-labeled dendrites in comparison to estrus females (Fig. 1F).

AIS effects on MOR trafficking in PARV-labeled dendrites

Regardless of their stage in the estrous cycle, AIS significantly decreased ($p<0.05$) the total number of MOR SIG particles in PARV-labeled dendrites in the hilus of females (Fig. 2A–C). This decrease was driven by a significant decrease ($p<0.01$) in the cytoplasmic density of MOR SIG particles in AIS females compared to control females (Fig. 2D). AIS did not alter the ratio of plasmalemma, near-plasmalemma or cytoplasmic to total MOR SIG particles in PARV-labeled dendrites in females (Fig. 2E).

Although no significant interaction between estrous cycle stage and AIS was observed by two-way ANOVA, we conducted further analysis by t-test to specifically assess the effect of AIS in proestrus females. In response to AIS, proestrus females displayed decreased cytoplasmic density ($p<0.05$; Fig. 2F) and increased plasmalemmal density ($p<0.05$; Fig. 2G) of MOR SIG particles in small (< 1.0 μm) PARV-labeled dendrites as compared to proestrus non-stressed controls. A similar analysis conducted in estrus females revealed a significant decrease ($p<0.01$) in cytoplasmic density, but not the plasmalemmal density, of MOR SIG particles in small PARV-labeled dendrites in response to AIS (Fig. 2F, G). No significant changes ($p> 0.05$) in MOR SIG particle density or proportions in large (> 1.0 μm) PARV-labeled dendrites were seen in either proestrus or estrus females after AIS (not shown).

AIS had different effects on MOR trafficking in PARV-labeled dendrites in males. AIS did not alter the total number of MOR SIG particles (Fig. 3A–C) or the density of MOR SIG particles on the plasmalemma or cytoplasm of PARV-labeled dendrites, regardless of size (Fig. 3D). In contrast, AIS significantly increased the ratio of cytoplasmic:total MOR SIG particles in PARV-labeled dendrites in males (Fig. 3E).

CIS effects on PARV neurons

In males, previous studies in rats and tree shrews (Czeh et al., 2005;Hu et al., 2010) have shown that chronic stress decreases the number of PARV-labeled neurons in the hilus of the rat dentate gyrus. It is unknown whether chronic stress similarly impacts PARV-labeled neurons in females. This is important as it would affect interpretation of electron microscopic assessment of MOR trafficking in PARV-labeled dendrites after CIS. Thus, we first counted the number of PARV-labeled neurons in the hilus of the dentate gyrus in females and males after CIS. PARV-immunoreactive cells were not counted in the region near CA3 as this region was not sampled in the electron microscopic studies. In agreement with earlier studies (Hu et al., 2010; Czeh et al., 2005), CIS significantly reduced the number of PARV-labeled cells in the dentate hilus of males by about 30% (Fig. 4A–C). In contrast, CIS did not significantly change the number of PARV-immunoreactive cells in females, regardless of estrous stage (Fig. 4C).

To determine if PARV-labeled neurons were degenerating after CIS, we next examined Fluoro-Jade staining in hippocampal sections from control and CIS males and estrus females. No Fluoro-Jade cells were detected in the dentate hilus from the control males and females and the CIS females. However, the dentate hilus from two out of the six CIS males each contained one Fluoro-Jade cell (not shown). Thus, this difference was not significant ($p > 0.05$). However, further ultrastructural analysis of the hilus of CIS males containing

Fluoro-Jade cells revealed 1–3 neurons (8–12 μm in diameter) with the morphological characteristics of degeneration: electron dense cytoplasm and homogeneous chromatin in the nuclei (Fig. 5A,B). The somata were localized in the subgranular hilus in the vicinity of PARV-labeled profiles (Fig. 5A,B) and received contacts from unlabeled terminals (Fig. 5A) . Electron dense dendritic profiles that were contacted by unlabeled terminals also were seen (Fig. 5C). Both degenerating somata and dendrites primarily were seen in the subgranular hilus; however, it was difficult to determine if they contained PARV-ir.

CIS effects on MOR trafficking in PARV dendrites

CIS had no effect on the length of the estrous cycle or the duration of the individual estrous phases. However, electron microscopic analysis of the hippocampus from CIS rats revealed striking sex differences. As seen with AIS, MOR SIG particles were found in the cytoplasm and on the plasmalemma of PARV-labeled dendrites and terminals in females (Figs. 6A,B and 8A,B) and males (not shown). However, only females had significant changes in the size of MOR-PARV dendrites and in the trafficking of MOR SIG particles in PARV-labeled dendrites.

Specifically, the area of MOR-PARV dendrites was significantly smaller ($p<0.05$) in CIS females compared to controls (Fig. 6C). Moreover, the density of MOR SIG particles in the cytoplasm (Fig. 6D) and on the plasmalemma (Fig. 6E) was significantly increased (<0.05) in the PARV-labeled dendrites of females. These changes were primarily driven by significant changes in the cytoplasmic density of MOR SIG particles in small (<1.0 μm in diameter) MOR-PARV dendrites (Fig. 6C–E). However, the cytoplasmic density of MOR SIG particles in large (>1.0 μm in diameter) MOR-PARV dendrites also tended to increase ($p = 0.06$). Additionally, the ratio of near-plasmalemma:total MOR SIG particles in large (>1.0 μm) PARV-labeled dendrites (Fig. 6F) was significantly reduced. In contrast, neither the area of MOR-PARV dendrites nor the density and partitioning ratios of MOR SIG particles in PARV-labeled dendrites changed significantly ($p>0.05$) in males (supplemental figure 1).

A similar sexual dimorphism was seen in the MOR-PARV terminals after CIS. Specifically, the area of MOR-PARV terminals was significantly smaller ($p<0.05$) in CIS females compared to controls (Fig. 7C). Moreover, the density of MOR SIG particles in the cytoplasm of PARV-labeled dendrites of CIS females was significantly increased ($p<0.05$; Fig. 7D). In contrast, neither the area of MOR-PARV terminals nor the density of MOR SIG particles in PARV-labeled terminals changed significantly ($p>0.05$) in males (Fig. 7E,F).

Discussion

This study demonstrates sex differences in the density and trafficking of MORs in hippocampal PARV-containing interneurons in response to stress (Fig. 8). In particular, the density of MORs in PARV-labeled dendrites is decreased in females and increased in males after AIS. Moreover, females display differences in the density of MORs on the plasmalemma and in the cytoplasm of PARV-labeled dendrites that are dependent on estrous cycle stage and AIS exposure. After CIS, males, but not females, had decreased numbers of PARV-labeled hilar neurons. Moreover, females have an increase in the density and alterations in the trafficking of MORs in PARV-labeled dendrites. Conversely, males have no change in either the size of MOR/PARV dendrites or the density or trafficking of MORs in PARV-labeled dendrites. These observed changes in MOR-PARV neurons may contribute to the reported sex differences in hippocampal-dependent behaviors in stressed animals, particularly learning relevant to drug abuse.

Methodological considerations

Similar to our earlier publication (Torres-Reveron et al., 2009b), this study utilized the pre-embedding immunogold-silver technique to localize MOR labeling. Although SIG labeling can produce lower estimates of receptor number than immunoperoxidase labeling, due to reduced reagent penetration (Leranth and Pickel, 1989), this limitation did not likely affect comparisons between groups since (a) hippocampal sections were pooled and processed together to control for differences in antibody penetration (Pierce et al., 1999), and (b) ultrathin sections were collected from the tissue-plastic interface where immunoreagent access is maximal (Milner et al., 2011). For each rat, we collected a similar number of dual labeled dendrites to insure that between-group comparisons were not affected by pre-embedding SIG limitations. By controlling these factors, variability between animals in each experimental group was minimal.

Our experiments were conducted in normal cycling animals as our previous studies (Torres-Reveron et al., 2008;Torres-Reveron et al., 2009a;Torres-Reveron et al., 2009b;Williams et al., 2011b) found robust differences in opioid peptide and receptor trafficking in different estrous cycle stages. In particular, proestrus rats have increased levels of enkephalins and dynorphins (Torres-Reveron et al., 2008, 2009a). We chose not to study the effects of stress in ovariectomized and estrogen replaced rats since we and others (Tanapat et al., 2005;Torres-Reveron et al., 2008;Torres-Reveron et al., 2009a;Torres-Reveron et al., 2009b) have found that the effects of estradiol vary depending on steroid dose, time elapsed after hormone administration, and interval following ovariectomy. For instance, our recent studies have shown that 3 days of estradiol treatment via silastic capsules either does not change or decreases the levels of leu-enkephalin levels and other synaptic proteins in the hippocampus (Williams et al., 2011a). Moreover, we did not want to introduce possible stress from multiple estradiol injections over the 10-day period.

The density of MOR-ir in PARV-labeled neurons differs with estrous cycle stage

In the dentate gyrus, MORs are found primarily in PARV-containing GABAergic basket interneurons which provide inhibitory inputs to the somata of granule cells (Drake et al., 2007). The present demonstration that the density and trafficking of MORs in PARV-labeled dendrites varies depending on estrous cycle stage is consistent with our earlier study (Torres-Reveron et al., 2009b). We previously focused on proestrus and diestrus females, as these are estrous cycle stages during which estrogen levels are highest and lowest, respectively (Turner and Bagnara, 1971) and found an increased density of MORs on the plasmalemma of PARV-labeled dendrites during proestrus (Torres-Reveron et al., 2009b). The present study included estrus females (when estrogens are declining and progestins are elevated) in the AIS experiments as this was the stage analyzed in the CIS rats by electron microscopy. We found that the density of MORs on the plasmalemma of PARV-labeled dendrites is even higher during estrus compared to proestrus in non-stressed (control) rats. A greater density of MORs on the plasmalemma would result in more receptors available for binding of endogenous ligands, e.g., enkephalin, or exogenous ligands, e.g., morphine (Boudin et al., 1998). Functionally, more available MORs can inhibit GABAergic neurons leading to augmented excitability and LTP at the mossy fiber-CA3 synapse (Akaishi et al., 2000;Derrick et al., 1992;Derrick and Martinez Jr., 1994). Importantly, enkephalins, which are released after high-frequency stimulation (Thureson-Klein and Klein, 1990), also are elevated in the mossy fibers at estrus and to a slightly lesser extent at proestrus (Torres-Reveron et al., 2008). Moreover, in the CA1 region of the hippocampus, the density of DORs on the plasmalemma of pyramidal cells is decreased in proestrus compared to diestrus rats (Williams et al., 2011b). Together, these findings suggest that opioid activation of the mossy fiber-CA3 synapse would be maximal at estrus and proestrus. Specifically, greater quantities of enkephalin would be released to bind to more available MORs on inhibitory

interneurons and fewer available DORs on pyramidal cells; as a result pyramidal cell excitation and LTP would be both indirectly and directly enhanced. This idea is strongly supported by our recent experiments showing that opioid-dependent LTP in the mossy fiber-CA3 synapse is greater in proestrus and estrus females compared to diestrus females and males (Varga-Wesson et al., 2011).

Following AIS, the density and trafficking of MORs varies with estrous cycle stage and sex

Regardless of estrous cycle stage, females had a decrease in the total density of MOR SIG particles in PARV-labeled dendrites following AIS that was driven by a decrease in cytoplasmic MORs. This decrease in MOR density after AIS was significant only in the smaller, presumably distal PARV-containing dendrites. However, when subdivided according to estrous cycle stage, only proestrus females had a greater density of MOR SIG particles on the plasmalemma of small PARV-labeled dendrites after AIS. The decrease in the total density of MOR SIG particles in PARV-labeled dendrites following AIS could represent a depletion of the reserve pools of MORs. Additionally, lack of change of MOR SIG particle density or distribution in the large PARV-labeled dendrites combined with the changes in cytoplasmic and plasmalemmal density of MOR SIG particles on small PARV-labeled dendrites likely indicates a trafficking of MORs towards the plasmalemma in the small dendrites in response to AIS when estrogen levels are highest. This would suggest that MORs are not internalized and that PARV-containing neurons in proestrus females may be less excitable in response to AIS. Alternatively or additionally, a movement of MORs to the plasmalemma may be a result of increased synaptic activity and could play a role in the early stages of neural plasticity as has been suggested for glutamate receptors (Bassani et al., 2009).

In contrast to females, males had no changes in either the total density of MOR SIG particles in PARV-labeled dendrites or in the density of MORs on the plasmalemma of PARV-labeled dendrites after AIS. However, males had an increased ratio of cytoplasmic:total MOR SIG particles in PARV-labeled small and large dendrites after AIS. This may suggest either an increased internalization of MORs or an increased trafficking of MORs from PARV-containing soma to their dendrites following AIS in males.

Overall, the changes in the density and trafficking of MOR SIG particles in PARV-labeled dendrites after AIS resulted in decreased MORs available for activation in females and increased MORs available for activation in males. These findings are consistent with our recent light microscopic study (Gonzales et al., 2011) demonstrating that AIS decreases phosphorylated MOR (pMOR) levels in the dentate gyrus of proestrus and estrus females but increases pMOR levels in males. Moreover, we also have found that AIS decreases pDOR levels in the CA2/3 region in estrus females but does not alter pDOR levels in males (Burstein et al., 2013). Together, these results suggest that AIS has opposite effects on the activation of hippocampal opioid receptors in females and males.

MORs in PARV-labeled interneurons and chronic stress

Although previous studies (Czeh et al., 2005;Hu et al., 2010) have shown that chronic stress decreases the number of PARV-labeled neurons in males, this is the first report to analyze the effect of CIS on PARV-labeled neurons in females. Interestingly, unlike in males, CIS did not result in a loss of PARV-labeled neurons in females, regardless of cycle stage. These findings are consistent with previous studies demonstrating that cycling rats fail to show chronic stress-induced CA3 dendritic retraction (McLaughlin et al., 2010). However, CIS does have some effect, as EM studies demonstrated that the overall size of large MOR-PARV dendrites was decreased by about 20% in females. Whether the PARV-containing

cells that remain in males after CIS have any unique morphological characteristics will be a subject of future investigation.

The decrease in PARV-labeled neurons in males after CIS could either indicate that PARV-labeled neurons are lost and/or PARV immunoreactivity has fallen below the level of detectability. The loss of at least some of the PARV-labeled interneurons is supported by ultrastructural detection of degenerating neurons in the subgranular hilus, which contains the majority of PARV-labeled neurons. It is important to note that the detection of degenerating neurons was highly variable between animals. Such variability was not unexpected, as other studies have found subsets of male rats to be more sensitive to chronic stress [reviewed by (Kabbaj, 2004)]. However, the failure to detect degenerating cells in the male CIS rats with Fluoro-Jade despite a noted decrease in PARV-labeled cells either indicates that PARV-ir is reduced below the level of detectability after CIS or that the time-point used in the current study for detecting degenerating cells is not optimal. Regardless, the present EM study sampled a subpopulation of PARV-labeled neurons in males that appears resistant to the deleterious effects of CIS.

Our electron microscopic studies revealed sex differences in the effects of CIS on the density and trafficking of MOR SIG particles in PARV-labeled dendrites in the dentate hilus. Specifically, the density of MOR SIG particles increased in PARV-labeled dendrites and the ratio of near-plasmalemma:total MOR SIG particles decreased in females after CIS. In contrast, CIS had no effect on the density and trafficking of MOR SIG particles in PARV-containing dendrites in males. In females, the density changes in large dendrites may primarily be due to the shrinkage in size: the area of large MOR-PARV dendrites decreased by about 17% whereas the total and cytoplasmic density of MOR SIG particles in large PARV-labeled dendrites increased by 25% and 18%, respectively. However, as with the males after AIS, the increased cytoplasmic density of MOR SIG particles in PARV-labeled dendrites could also be due to trafficking of MORs from the soma. This is more likely the case for the small PARV-containing dendrites, since no changes in their size were seen after CIS. The changes in the partitioning ratio of MOR SIG particles in PARV-labeled dendrites in females after CIS likely represent a redistribution of the MOR SIG particles in PARV-containing dendrites. In particular, reductions in near-plasmalemmal MOR SIG particles may indicate that the reserve pool of MORs is depleted after repeated exposure to stress.

MOR-PARV labeled terminals also had sexually dimorphic responses to CIS. In CIS females, the area of MOR-PARV terminals was reduced by about 22% and the density of MOR SIG particles in PARV-labeled terminals was increased by about 30%. Neither of these changes was seen in males after CIS. As discussed above, the changes in MOR density could be due to terminal shrinkage or increased trafficking of MORs from the soma.

Functional considerations

The current findings support a growing body of literature that the effects of stress on the brain systems involved in learning are sexually dimorphic [reviewed in (Bangasser et al., 2010;Luine et al., 2007)]. The present study revealed that AIS and CIS alter the density and trafficking of MORs in hippocampal PARV neurons in opposing directions in females and males. Moreover, after CIS the number of PARV-labeled cells decreased in males, but not females. These changes could have important implications for hippocampal function.

Hippocampal PARV cells, which contain the majority of MORs (Drake and Milner, 2006), are a subpopulation of GABAergic interneurons that innervate pyramidal and granule cells (Freund and Buzsáki, 1996) and, to a lesser extent, cholecystokinin interneurons (Karson et al., 2009). Agonist activation of hippocampal MORs inhibits GABAergic transmission, producing net excitation and facilitation of LTP [reviewed by (Drake et al., 2007)]. Our

findings in males would suggest that the disinhibitory function of MORs on PARV neurons is maintained or even enhanced following AIS but disrupted following CIS. This assertion is supported by the findings in male rats that 21 days of chronic restraint stress impairs rhythmic firing of PARV interneurons (Hu et al., 2010). Conversely, our findings in females suggest that the MOR-activated disinhibition of PARV neurons may be diminished following AIS but is not changed or even potentially increased following CIS. As a result, the facilitation of LTP would be predicted to be maintained or even enhanced in females, but not males, following chronic stress.

In the dentate gyrus, MOR-PARV terminals primarily arise from intrinsic GABAergic-basket cells (Drake et al., 2007) and, to a lesser extent, from GABAergic septal neurons (Alreja et al., 2000). The increased density of MOR SIG particles in PARV terminals after CIS could affect synaptic transmission from both of these sources. In particular, presynaptic MORs are involved in regulation of delayed rectifying potassium channels (Wimpey and Chavkin, 1991), voltage-sensitive calcium channels (Herlitze et al., 1996;Ikeda, 1996) and vesicular fusion machinery (Capogna et al., 1996;Scholz and Miller, 1992).

In conclusion, these data show that AIS and CIS differentially affect available MOR pools in PARV-containing interneurons in female and male rats. Moreover, they suggest that CIS could affect CA3 pyramidal cell excitability in a manner that maintains learning processes in females but not males. These sex differences in the network properties of MOR-PARV could play a role in differences in learning following acute and chronic stress (Luine et al., 2007) and in the accelerated course of addiction seen in females (Elman et al., 2001;Hu et al., 2004;Lynch et al., 2000;Robbins et al., 1999).

Supplementary Material

Refer to Web version on PubMed Central for supplementary material.

Acknowledgments

We thank Dr. Karen Bulloch (The Rockefeller University) for the use of her Nikon H550L microscope. The authors have no conflict of interest to declare.

GRANT SUPPORT: NIH grants DA08259, HL098351 & HL096571 (TAM), MSTP grant GM07739 (TJW), NS007080 (BSM) and DK07313 & AG059850 (EMW)

References

Abbadie C, Pan YX, Drake CT, Pasternak GW. Comparative immunohistochemical distributions of carboxy terminus epitopes from the mu-opioid receptor splice variants MOR-1D, MOR-1 and MOR-1C in the mouse and rat CNS. Neurosci. 2000; 100:141–153.

Akaishi T, Saito H, Ito Y, Ishige K, Ikegaya Y. Morphine augments excitatory synaptic transmission in the dentate gyrus through GABAergic disinhibition. Neurosci Res. 2000; 38:357–363. [PubMed: 11164562]

Alreja M, Shanabrough M, Liu WM, Leranth C. Opioids suppress IPSCs in neurons of the rat medial septum/diagonal band of Broca: Involvement of m-opioid receptors and septohippocampal GABAergic neurons. J Neurosci. 2000; 20:1179–1189. [PubMed: 10648722]

Arvidsson U, Riedl M, Chakrabarti S, Lee JH, Nakano AH, Dado RJ, Loh HH, Law PY, Wessendorf MW, Elde R. Distribution and targeting of a mu-opioid receptor (MOR1) in brain and spinal cord. J Neurosci. 1995; 15:3328–3341. [PubMed: 7751913]

Atkins AL, Mashhoon Y, Kantak KM. Hippocampal regulation of contextual cue-induced reinstatement of cocaine-seeking behavior. Pharmacol Biochem Behav. 2008; 90:481–491. [PubMed: 18499239]

Bangasser DA, Curtis A, Reyes BA, Bethea TT, Parastatidis I, Ischiropoulos H, Van Bockstaele EJ, Valentino RJ. Sex differences in corticotropin-releasing factor receptor signaling and trafficking: potential role in female vulnerability to stress-related psychopathology. Mol Psychiatry. 2010; 15 877, 896-877, 904.

Bassani S, Valnegri P, Beretta F, Passafaro M. The GLUR2 subunit of AMPA receptors: synaptic role. Neuroscience. 2009; 158:55–61. [PubMed: 18977416]

Becker JB, Monteggia LM, Perrot-Sinal TS, Romeo RD, Taylor JR, Yehuda R, Bale TL. Stress and disease: is being female a predisposing factor? J Neurosci. 2007; 27:11851–11855. [PubMed: 17978023]

Bossert JM, Poles GC, Wihbey KA, Koya E, Shaham Y. Differential effects of blockade of dopamine D1-family receptors in nucleus accumbens core or shell on reinstatement of heroin seeking induced by contextual and discrete cues. J Neurosci. 2007; 27:12655–12663. [PubMed: 18003845]

Boudin H, Pélaprat D, Rostène W, Pickel VM, Beaudet A. Correlative ultrastructural distribution of neurotensin receptor proteins and binding sites in the rat substantia nigra. J Neurosci. 1998; 18:8473–8484. [PubMed: 9763490]

Bowman RE, Beck KD, Luine VN. Chronic stress effects on memory: sex differences in performance and monoaminergic activity. Horm Behav. 2003; 43:48–59. [PubMed: 12614634]

Bruchas MR, Xu M, Chavkin C. Repeated swim stress induces kappa opioid-mediated activation of extracellular signal-regulated kinase 1/2. Neuroreport. 2008; 19:1417–1422. [PubMed: 18766023]

Burstein SR, Williams TJ, Lane DA, Knudson MG, Pickel VM, McEwen BS, Waters EM, Milner TA. The influences of reproductive status and acute stress on the levels of phosphorylated delta opioid receptor immunoreactivity in the rat hippocampus. Brain Res in press. 2013

Capogna M, Gahwiler BH, Thompson SM. Presynaptic inhibition of calcium-dependent and -independent release elicited with ionomycin, gadolinium, and alpha-latrotoxin in the hippocampus. J Neurophysiol. 1996; 75:2017–2028. [PubMed: 8734600]

Celio MR. Calbindin D-28k and parvalbumin in the rat nervous system. Neurosci. 1990; 35:375–475.

Conrad CD, Grote KA, Hobbs RJ, Ferayorni A. Sex differences in spatial and non-spatial Y-maze performance after chronic stress. Neurobiol Learn Mem. 2003; 79:32–40. [PubMed: 12482677]

Crombag HS, Bossert JM, Koya E, Shaham Y. Review. Context-induced relapse to drug seeking: a review. Philos Trans R Soc Lond B Biol Sci. 2008; 363:3233–3243. [PubMed: 18640922]

Czeh B, Simon M, van der Hart MG, Schmelting B, Hesselink MB, Fuchs E. Chronic stress decreases the number of parvalbumin-immunoreactive interneurons in the hippocampus: prevention by treatment with a substance P receptor (NK1) antagonist. Neuropsychopharmacology. 2005; 30:67–79. [PubMed: 15470372]

Derrick BE, Martinez JL Jr. Opioid receptor activation is one factor underlying the frequency dependence of mossy fiber LTP induction. J Neurosci. 1994; 14:4359–4367. [PubMed: 7913121]

Derrick BE, Rodriguez SB, Lieberman DN, Martinez JL Jr. Mu opioid receptors are associated with the induction of hippocampal mossy fiber long-term potentiation. J Pharmacol Exp Ther. 1992; 263:725–733. [PubMed: 1359112]

Drake CT, Chang PC, Harris JA, Milner TA. Neurons with mu opioid receptors interact indirectly with enkephalin-containing neurons in the rat dentate gyrus. Exp Neurol. 2002; 176:254–261. [PubMed: 12093103]

Drake CT, Chavkin C, Milner TA. Opioid systems in the dentate gyrus. Prog Brain Res. 2007; 163:245–814. [PubMed: 17765723]

Drake CT, Milner TA. Mu opioid receptors are in somatodendritic and axonal compartments of GABAergic neurons in rat hippocampal formation. Brain Res. 1999; 849:203–215. [PubMed: 10592303]

Drake CT, Milner TA. Mu opioid receptors are extensively co-localized with parvalbumin, but not somatostatin, in the dentate gyrus. Neurosci Lett. 2006; 403:176–180. [PubMed: 16716508]

Elman I, Karlsgodt KH, Gastfriend DR. Gender differences in cocaine craving among non-treatment-seeking individuals with cocaine dependence. Am J Drug Alcohol Abuse. 2001; 27:193–202. [PubMed: 11417935]

Fiorentine R, Anglin MD, Gil-Rivas V, Taylor E. Drug treatment: explaining the gender paradox. Subst Use Misuse. 1997; 32:653–678. [PubMed: 9178435]

Freund TF, Buzsáki G. Interneurons of the hippocampus. Hippocampus. 1996; 6:347–470. [PubMed: 8915675]

Galea LAM, McEwen BS, Tanapat P, Deak T, Spencer RL, Dhabhar FS. Sex differences in dendritic atrophy of CA3 pyramidal neurons in response to chronic restraint stress. Neurosci. 1997; 81:689–697.

Gerrits MA, Lesscher HB, van Ree JM. Drug dependence and the endogenous opioid system. Eur Neuropsychopharmacol. 2003; 13:424–434. [PubMed: 14636958]

Gonzales KL, Chapleau JD, Pierce JP, Kelter DT, Williams TJ, Torres-Reveron A, McEwen BS, Waters EM, Milner TA. The influences of reproductive status and acute stress on the levels of phosphorylated mu opioid recetpor immunoreactivity in rat hippocampus. Front Neuroendocrinol. 2011; 2:1–10.

Herlitze S, Garcia DE, Mackie K, Hille B, Scheuer T, Catterall WA. Modulation of Ca2+ channels by G-protein beta gamma subunits. Nature. 1996; 380:258–262. [PubMed: 8637576]

Hu M, Crombag HS, Robinson TE, Becker JB. Biological basis of sex differences in the propensity to self-administer cocaine. Neuropsychopharmacology. 2004; 29:81–85. [PubMed: 12955098]

Hu W, Zhang M, Czeh B, Flugge G, Zhang W. Stress impairs GABAergic network function in the hippocampus by activating nongenomic glucocorticoid receptors and affecting the integrity of the parvalbumin-expressing neuronal network. Neuropsychopharmacology. 2010; 35:1693–1707. [PubMed: 20357756]

Hyman SE, Malenka RC. Addiction and the brain: the neurobiology of compulsion and its persistence. Nat Rev Neurosci. 2001; 2:695–703. [PubMed: 11584307]

Ikeda SR. Voltage-dependent modulation of N-type calcium channels by G-protein beta gamma subunits. Nature. 1996; 380:255–258. [PubMed: 8637575]

Kabbaj M. Neurobiological bases of individual differences in emotional and stress responsiveness: high responders-low responders model. Arch Neurol. 2004; 61:1009–1012. [PubMed: 15262729]

Karson MA, Tang AH, Milner TA, Alger BE. Synaptic cross talk between perisomatic-targeting interneuron classes expressing cholecystokinin and parvalbumin in hippocampus. J Neurosci. 2009; 29:4140–4154. [PubMed: 19339609]

Kilts CD, Schweitzer JB, Quinn CK, Gross RE, Faber TL, Muhammad F, Ely TD, Hoffman JM, Drexler KP. Neural activity related to drug craving in cocaine addiction. Arch Gen Psychiatry. 2001; 58:334–341. [PubMed: 11296093]

Kitraki E, Kremmyda O, Youlatos D, Alexis MN, Kittas C. Gender-dependent alterations in corticosteroid receptor status and spatial performance following 21 days of restraint stress. Neuroscience. 2004; 125:47–55. [PubMed: 15051144]

Koob GF. A role for brain stress systems in addiction. Neuron. 2008; 59:11–34. [PubMed: 18614026]

Leranth, C.; Pickel, VM. Electron microscopic preembedding double-labeling methods. In: Heimer, L.; Zaborszky, L., editors. Neuroanatomical Tract-Tracing Methods 2. New York: Plenum Press; 1989. p. 129-172.

Leshner AI. Prescription drugs: Abuse and addiction. NIDA Research Report. 2002; 1:1–12.

Lucas LR, Wang CJ, McCall TJ, McEwen BS. Effects of immobilization stress on neurochemical markers in the motivational system of the male rat. Brain Res. 2007; 1155:108–115. [PubMed: 17511973]

Luine VN, Beck KD, Bowman RE, Frankfurt M, MacLusky NJ. Chronic stress and neural function: accounting for sex and age. J Neuroendocrinol. 2007; 19:743–751. [PubMed: 17850456]

Luo AH, Tahsili-Fahadan P, Wise RA, Lupica CR, Aston-Jones G. Linking context with reward: a functional circuit from hippocampal CA3 to ventral tegmental area. Science. 2011; 333:353–357. [PubMed: 21764750]

Lynch WJ, Arizzi MN, Carroll ME. Effects of sex and the estrous cycle on regulation of intravenously self-administered cocaine in rats. Psychopharmacology (Berl). 2000; 152:132–139. [PubMed: 11057516]

Magarinos AM, Verdugo JM, McEwen BS. Chronic stress alters synaptic terminal structure in hippocampus. Proc Natl Acad Sci U S A. 1997; 94:14002–14008. [PubMed: 9391142]

McEwen BS. Stress and hippocampal plasticity. Annu Rev Neurosci. 1999; 22:105–122. [PubMed: 10202533]

McEwen BS, Milner TA. Hippocampal formation: shedding light on the influence of sex and stress on the brain. Brain Res Rev. 2007; 55:343–355. [PubMed: 17395265]

McLaughlin JP, Marton-Popovici M, Chavkin C. Kappa opioid receptor antagonism and prodynorphin gene disruption block stress-induced behavioral responses. J Neurosci. 2003; 23:5674–5683. [PubMed: 12843270]

McLaughlin KJ, Wilson JO, Harman J, Wright RL, Wieczorek L, Gomez J, Korol DL, Conrad CD. Chronic 17beta-estradiol or cholesterol prevents stress-induced hippocampal CA3 dendritic retraction in ovariectomized female rats: possible correspondence between CA1 spine properties and spatial acquisition. Hippocampus. 2010; 20:768–786. [PubMed: 19650122]

Milner, TA.; Waters, EM.; Robinson, DC.; Pierce, JP. Degenerating processes identified by electron microscpic immunocytochemical methods. In: Manfredi, G.; Kawamata, H., editors. Neurodegeneration, Methods and Protocols. New York: Springer; 2011. p. 23-59.

Nestler EJ. Molecular basis of long-term plasticity underlying addiction. Nat Rev Neurosci. 2001; 2:119–128. [PubMed: 11252991]

Peters, A.; Palay, SL.; Webster, Hd. The fine structure of the nervous system. 3rd ed.. New York: Oxford University Press; 1991.

Pham K, Nacher J, Hof PR, McEwen BS. Repeated restraint stress suppresses neurogenesis and induces biphasic PSA-NCAM expression in the adult rat dentate gyrus. Eur J Neurosci. 2003; 17:879–886. [PubMed: 12603278]

Ribak CE, Nitsch R, Seress L. Proportion of parvalbumin-positive basket cells in the GABAergic innervation of pyramidal and granule cells of the rat hippocampal formation. J Comp Neurol. 1990; 300:449–461. [PubMed: 2273087]

Risinger FO, Oakes RA. Nicotine-induced conditioned place preference and conditioned place aversion in mice. Pharmacol Biochem Behav. 1995; 51:457–461. [PubMed: 7667368]

Robbins SJ, Ehrman RN, Childress AR, O'Brien CP. Comparing levels of cocaine cue reactivity in male and female outpatients. Drug Alcohol Depend. 1999; 53:223–230. [PubMed: 10080048]

Rogers JL, Ghee S, See RE. The neural circuitry underlying reinstatement of heroin-seeking behavior in an animal model of relapse. Neuroscience. 2008; 151:579–588. [PubMed: 18061358]

Schmued LC, Albertson C, Slikker W Jr. Fluoro-Jade: A novel fluorochrome for the sensitive and reliable histochemical localization of neuronal degeneration. Brain Res. 1997; 751:37–46. [PubMed: 9098566]

Scholz KP, Miller RJ. Inhibition of quantal transmitter release in the absence of calcium influx by a G protein-linked adenosine receptor at hippocampal synapses. Neuron. 1992; 8:1139–1150. [PubMed: 1351733]

Shalev U, Highfield D, Yap J, Shaham Y. Stress and relapse to drug seeking in rats: studies on the generality of the effect. Psychopharmacology (Berl). 2000; 150:337–346. [PubMed: 10923762]

Shansky RM, Hamo C, Hof PR, Lou W, McEwen BS, Morrison JH. Estrogen promotes stress sensitivity in a prefrontal cortex-amygdala pathway. Cereb Cortex. 2010; 20:2560–2567. [PubMed: 20139149]

Simmons ML, Chavkin C. Endogenous opioid regulation of hippocampal function. Int Rev Neurobiol. 1996; 39 145-96 145–196.

Skyers PS, Einheber S, Pierce JP, Milner TA. Increased mu-opioid receptor labeling is found on inner molecular layer terminals of the dentate gyrus following seizures. Exp Neurol. 2003; 179:200–209. [PubMed: 12618127]

Tanapat P, Hastings NB, Gould E. Ovarian steroids influence cell proliferation in the dentate gyrus of the adult female rat in a dose- and time-dependent manner. J Comp Neurol. 2005; 481:252–265. [PubMed: 15593136]

Thureson-Klein AK, Klein RL. Exocytosis from neuronal large dense-core vesicles. Int Rev Cytol. 1990; 121:67–126. [PubMed: 1972143]

Torres-Reveron A, Khalid S, Williams TJ, Waters EM, Drake CT, McEwen BS, Milner TA. Ovarian steroids modulate leu-enkephalin levels and target leu-enkephalinergic profiles in the female hippocampal mossy fiber pathway. Brain Res. 2008; 1232:70–84. 70–84. [PubMed: 18691558]

Torres-Reveron A, Khalid S, Williams TJ, Waters EM, Jacome L, Luine VN, Drake CT, McEwen BS, Milner TA. Hippocampal dynorphin immunoreactivity increases in response to gonadal steroids

and is positioned for direct modulation by ovarian steroid receptors. Neurosci. 2009a; 159:204–216.

Torres-Reveron A, Williams TJ, Chapleau JD, Waters EM, McEwen BS, Drake CT, Milner TA. Ovarian steroids alter mu opioid receptor trafficking in hippocampal parvalbumin GABAergic interneurons. Exp Neurol. 2009b; 219:319–327. [PubMed: 19505458]

Turner, CD.; Bagnara, JT. General Endocrinology. Philadelphia: W.B. Saunders; 1971.

Varga-Wesson, A.; Harte, LC.; Milner, TA.; MacLusky, NJ.; Scharfman, HE. Program no. 869.02 2011 Meeting Planner. Washington, DC: Society for Neuroscience; 2011. Differences in mossy fiber plasticity in adult male and remale rat hippocampal slices. 2011. Online

Volkow ND, Wang GJ, Telang F, Fowler JS, Logan J, Childress AR, Jayne M, Ma Y, Wong C. Cocaine cues and dopamine in dorsal striatum: mechanism of craving in cocaine addiction. J Neurosci. 2006; 26:6583–6588. [PubMed: 16775146]

Vorel SR, Liu X, Hayes RJ, Spector JA, Gardner EL. Relapse to cocaine-seeking after hippocampal theta burst stimulation. Science. 2001; 292:1175–1178. [PubMed: 11349151]

Vyas A, Mitra R, Shankaranarayana Rao BS, Chattarji S. Chronic stress induces contrasting patterns of dendritic remodeling in hippocampal and amygdaloid neurons. J Neurosci. 2002; 22:6810–6818. [PubMed: 12151561]

Weiss RD, Martinez-Raga J, Griffin ML, Greenfield SF, Hufford C. Gender differences in cocaine dependent patients: a 6 month follow-up study. Drug Alcohol Depend. 1997; 44:35–40. [PubMed: 9031818]

Williams TJ, Milner TA. Delta opioid receptors colocalize with corticotropin releasing factor in hippocampal interneurons. Neuroscience. 2011; 179:9–22. [PubMed: 21277946]

Williams TJ, Mitterling KL, Thompson LI, Torres-Reveron A, Waters EM, McEwen BS, Gore AC, Milner TA. Age- and hormone-regulation of opioid peptides and synaptic proteins in the rat dorsal hippocampal formation. Brain Res. 2011a; 1379:71–85. [PubMed: 20828542]

Williams TJ, Torres-Reveron A, Chapleau JD, Milner TA. Hormonal regulation of delta opioid receptor immunoreactivity in interneurons and pyramidal cells in the rat hippocampus. Neurobiol Learn Mem. 2011b; 95:206–220. [PubMed: 21224009]

Wimpey TL, Chavkin C. Opioids activate both an inward rectifier and a novel voltage-gated potassium conductance in the hippocampal formation. Neuron. 1991; 6:281–289. [PubMed: 1993123]

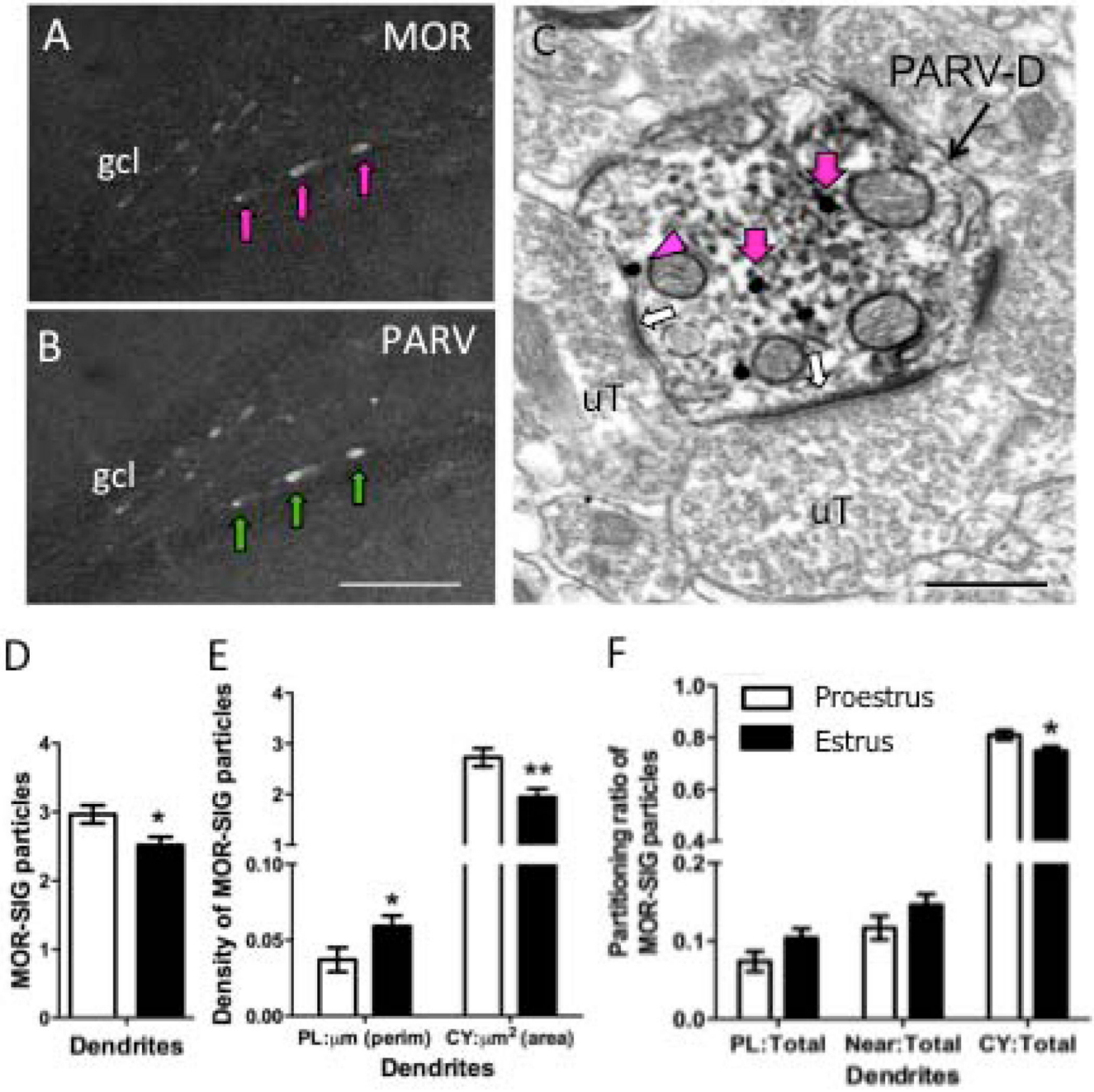

Figure 1. Ovarian hormones influence MOR subcellular distribution in PARV-labeled dendrites in the hilus

Light micrographs show MOR-ir alone (**A**) and PARV-ir alone (**B**) from the hilus of the dentate gyrus of a proestrus female rat. Arrows indicate examples of cells that contain both MOR- and PARV-labels. **C**. Electron micrograph showing an example of a PARV-labeled dendrite (PARV-D) that contains MOR SIG particles in the cytoplasm (magenta arrows) or on the plasma membrane (magenta arrowhead) from a proestrus rat. Unlabeled terminals (uT) form asymmetric synapses (white arrows) on the dendrite. Scale bars A, B = 50 μm; C = 500 nm. **D**. Significantly fewer total MOR SIG particles are in PARV-labeled dendrites in estrus females compared to proestrus females. **E**. Both proestrus and estrus females have a

greater density of MOR SIG particles in the cytoplasm compared to the plasma membrane. However, estrus females have significantly more MOR SIG particles on the plasma membrane (*$p < 0.05$) and fewer MOR-SIG particles (**$p < 0.001$) in the cytoplasm of PARV-labeled dendrites. **F**. Proestrus females showed an increased distribution of MOR SIG particles to the cytoplasm of PARV-labeled dendritic profiles in comparison to estrus females (*$p<0.05$).

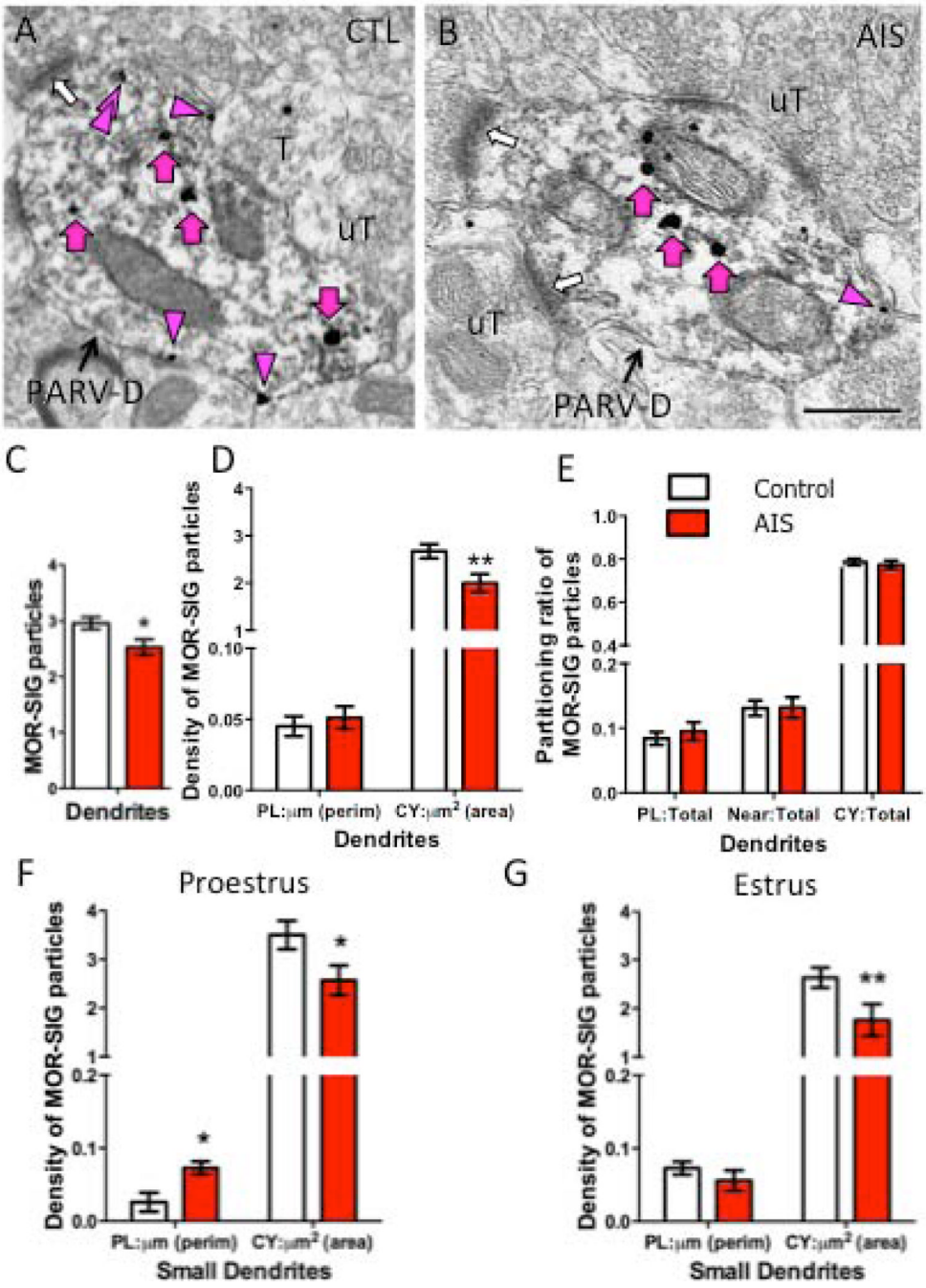

Figure 2. AIS reduces the number and density of MOR SIG particles in PARV-labeled dendrites in female rats

Examples of PARV-labeled dendrites (PARV-D) containing MOR SIG particles in the cytoplasm (magenta arrows), on the plasma membrane (magenta arrowhead) and near the plasma membrane (double magenta arrowheads) from control (**A**) and AIS (**B**) proestrus females. Unlabeled terminals (uT) contact (white arrows) dual labeled dendrites. Scale bars = 500 nm. **C**. AIS significantly decreased the total number of MOR SIG particles in PARV-labeled dendrites of females, regardless of their stage in the estrous cycle (*$p < 0.05$). **D**. AIS significantly reduced the cytoplasmic density of MOR SIG particles in PARV-labeled dendrites of females, regardless of estrous cycle stage (**$p < 0.01$). **E**. AIS did not alter

MOR SIG particle distribution on the plasma membrane, near the plasma membrane, or in the cytoplasm of PARV-labeled dendrites ($p > 0.05$), regardless of estrous cycle stage. **F, G**. After AIS, proestrus females displayed increased plasma membrane density ($*p < 0.05$; **F**) and decreased cytoplasmic density ($*p < 0.05$; **G**) of MOR SIG particles in small PARV-labeled dendrites whereas estrus females had a significant decrease in cytoplasmic density of MOR SIG particles in small PARV-labeled dendrites ($**p < 0.01$; **G**). N = 3 rats per group; n = 50 dendrites per rat

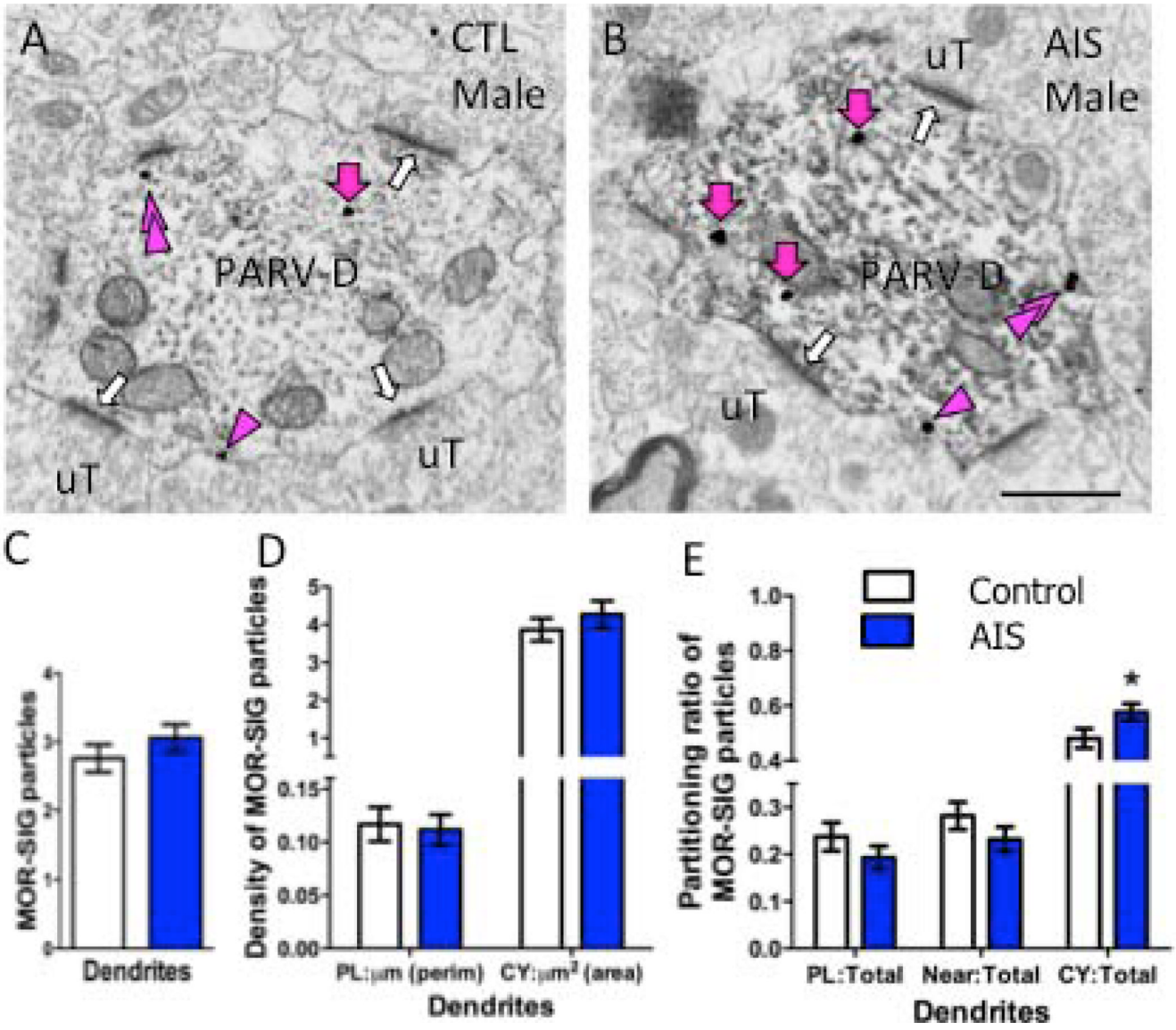

Figure 3. AIS increases the density of MOR SIG particles in PARV dendrites in male rats

Examples of PARV-labeled dendrites (PARV-D) containing MOR SIG particles in the cytoplasm (magenta arrows), on the plasma membrane (magenta arrowhead) and near the plasma membrane (double magenta arrowheads) from control (**A**) and AIS (**B**) male rats. Unlabeled terminals (uT) contact (white arrows) dual labeled dendrites. Scale bars = 500 nm. **C, D**. AIS did not alter the total number (**C**) or the plasma membrane and cytoplasmic density of MOR SIG particles (**D**) in PARV-labeled dendrites of males ($p>0.05$). **E**. AIS increased the MOR SIG particle distribution to the cytoplasm of PARV-labeled dendrites (*$p < 0.05$) in males. N = 3 rats per group; n = 50 dendrites per rat

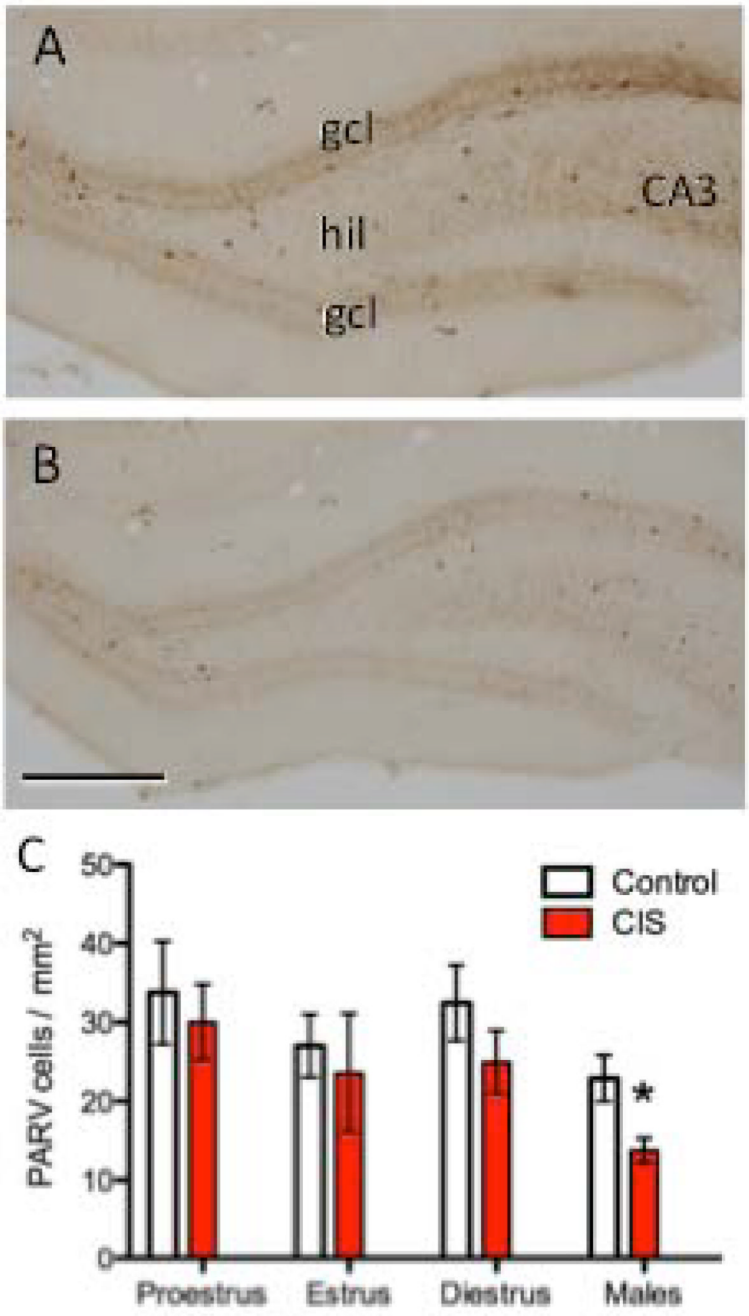

Figure 4. CIS decreases the number of PARV-labeled cells in the hilus of male, but not female, rats

Representative photomicrographs show the distribution of PARV-labeled cells in the dentate gyrus from control (**A**) and CIS (**B**) male rats. CA3, cornu ammonis 3 region; gcl, granule cell layer; hil, hilus. Scale bar = 50 μm. **C**. The number of PARV-labeled cells was not significantly different in CIS and control female rats, regardless of estrous stage. Conversely, the number of PARV-labeled cells was significantly less (*$p < 0.05$) in CIS compared to control males. N = 6 rats per group.

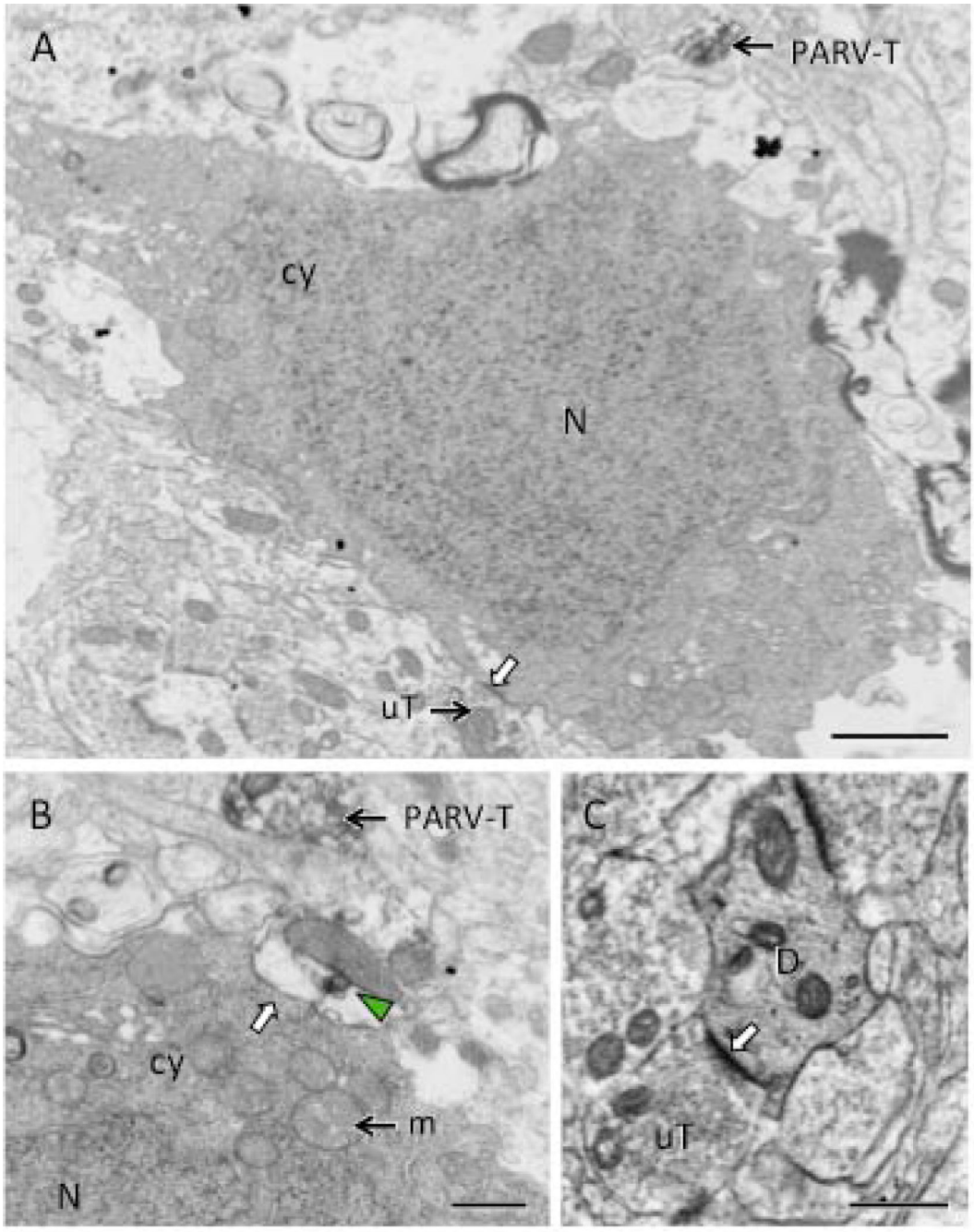

Figure 5. Electron microscopy reveals necrotic cell profiles in the hilus of male CIS rats

A. A neuronal cell body, identified by its size and the presence of unlabeled terminals (uT) synapsing on the plasma membrane (white arrow), contains a dark nucleus (N) and dark cytoplasm (cy). A PARV-labeled terminal (PARV-T) is found nearby. **B**. At high magnification, a swollen profile with a patch of PARV-labeling (green arrowhead) abuts (white arrow) another neuron cell body with dark cytoplasm (cy) and nucleus (N). A PARV-labeled terminal (PARV-T) is found nearby. Numerous swollen mitochondria (m) are found in the cytoplasm of the profiles in **A** and **B. C**. A dendrite (D) with dark cytoplasm is contacted (white arrow) by an unlabeled terminal (uT). Scale bars = 500 nm.

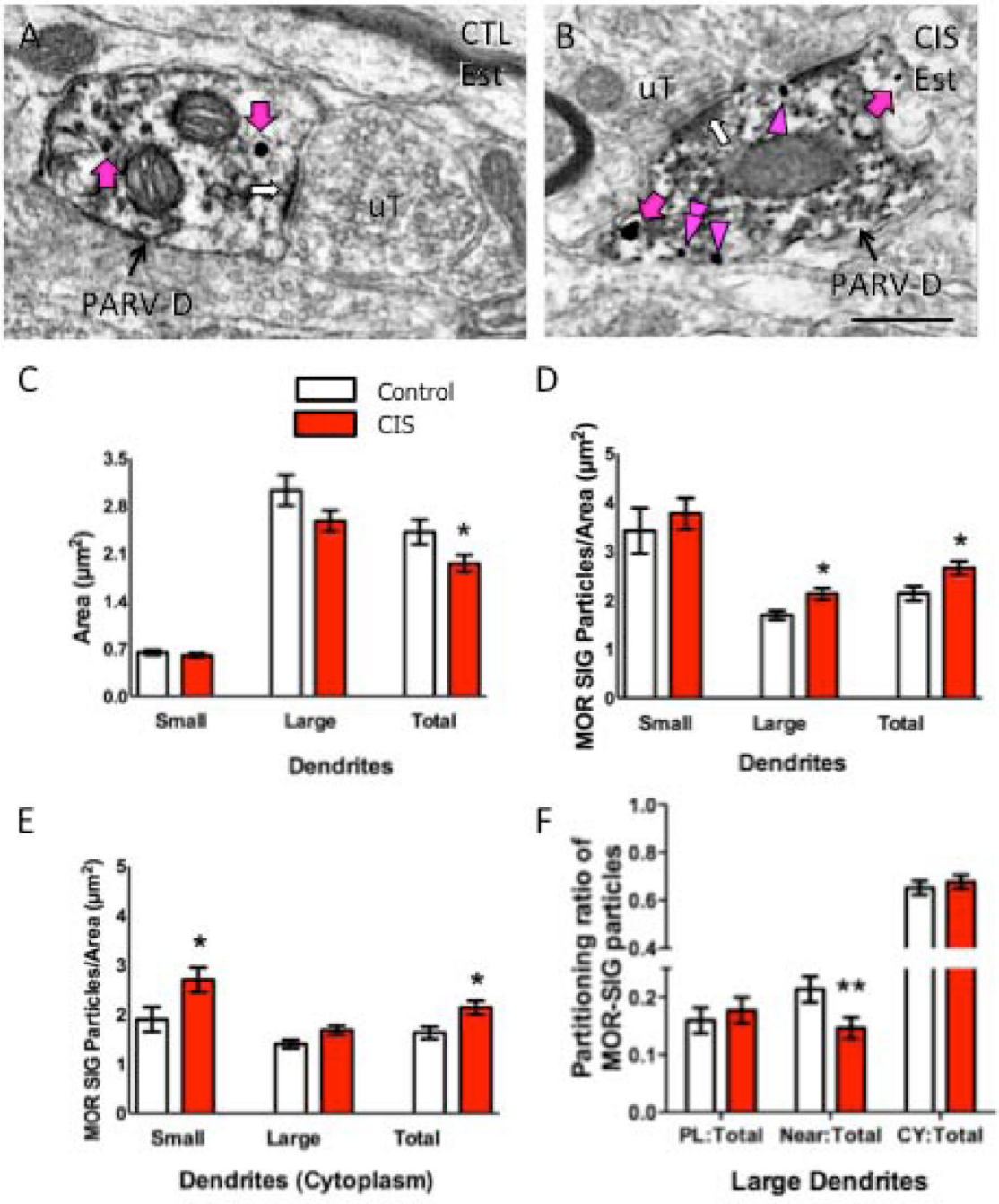

Figure 6. CIS affects the number and density of MOR SIG particles in PARV-labeled dendrites in female rats

Examples of PARV-labeled dendrites (PARV-D) containing MOR SIG particles in the cytoplasm (magenta arrows), on the plasma membrane (magenta arrowhead) and near the plasma membrane (double magenta arrowheads) from control (**A**) and CIS (**B**) estrus females. Unlabeled terminals (uT) contact (white arrows) dual labeled dendrites. Scale bars = 500 nm. **C**. Following CIS, the area of total PARV-labeled dendrites was less (*$p < 0.05$) and tended to be less in large dendrites ($p = 0.06$) in CIS estrus females compared to controls. **D**. CIS significantly increased the total density of MOR SIG particles in large and total PARV-labeled dendrites of estrus females (*$p < 0.05$). **E**. CIS significantly increased

(*$p < 0.05$) the cytoplasmic density of MOR SIG particles in small and total PARV-labeled dendrites and tended ($p = 0.06$) to increase the cytoplasmic density of MOR SIG particles in large PARV-labeled dendrites. **F**. CIS significantly decreased (**$p < 0.01$) the near plasma membrane MOR SIG particle distribution in of PARV-labeled dendrites in estrus females. N = 3 rats per group; n = 50 dendrites per rat.

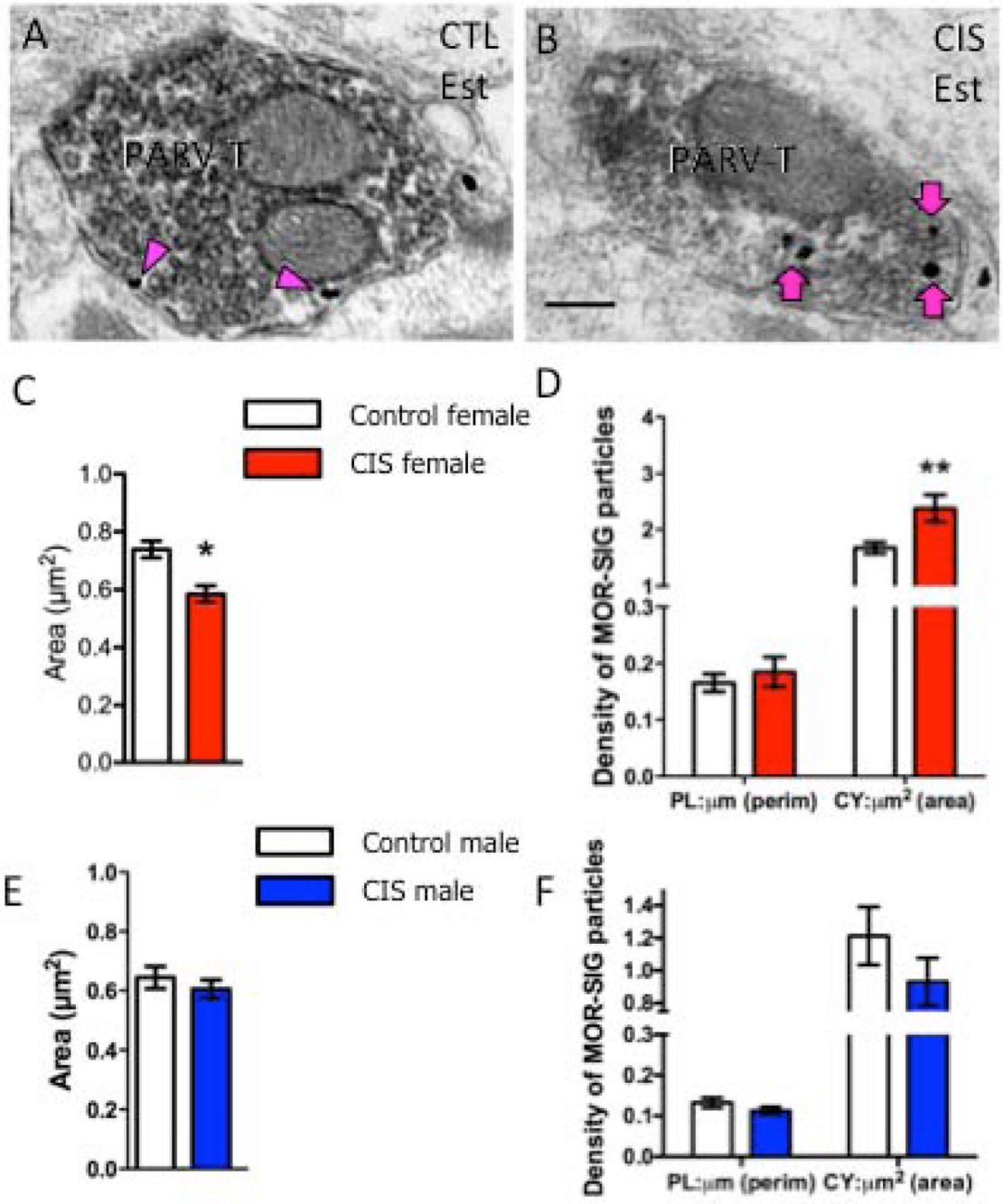

Figure 7. CIS affects the number and density of MOR SIG particles in PARV-labeled terminals in female, but not male, rats

Examples of PARV-labeled terminals (PARV-T) containing MOR SIG particles in the cytoplasm (magenta arrows) and on the plasma membrane (magenta arrowhead) from control (**A**) and CIS (**B**) estrus females. Scale bars = 500 nm. **C**. Following CIS, the area of PARV-labeled terminals was significantly less (*$p < 0.05$) in CIS estrus females compared to controls. **D**. CIS significantly increased the cytoplasmic density of MOR SIG particles in PARV-labeled terminals of females (**$p < 0.01$). **E**. Following CIS, the area of PARV-labeled terminals was not significantly different ($p > 0.05$) in CIS males compared to controls. **F**. No significant differences were seen in either the plasma membrane or

cytoplasmic density of MOR SIG particles in PARV-labeled terminals of CIS and control males ($p > 0.05$). N = 3 rats per group; n = 30–50 terminals per rat.

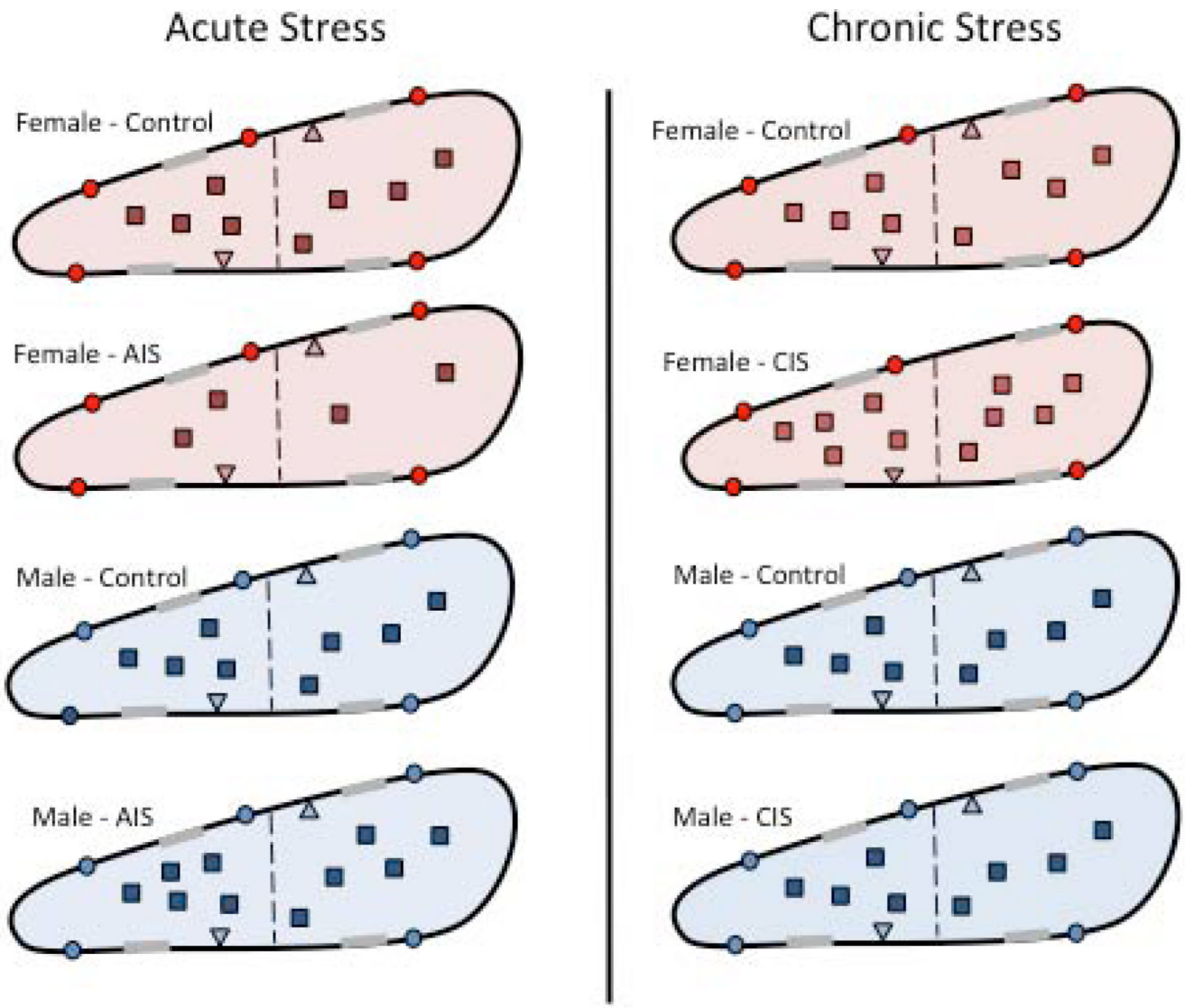

Figure 8. Schematic diagram summarizing the effects of acute and chronic stress on the density and trafficking of MORs in PARV dendrites in the hippocampus of female and male rats

MORs are located on the plasmalemma (circle), near-plasmalemma (triangle) and in the cytoplasm (square) of PARV-containing dendrites in female and male rats. For ease of comparison, only estrus females are shown. Dashed line indicated division between small and large PARV-labeled dendrites and gray shadings on membranes indicate synapses. After AIS, fewer MORS are detected in the cytoplasm of small PARV-containing dendrites in females (red) whereas the proportion of MORs in cytoplasm compared to the total is greater in small and large PARV-containing dendrites in males (blue). After CIS, the numbers of PARV-labeled neurons decrease by about 30% in males but do not change in females (not shown). However, the size of large PARV-labeled dendrites decreases about 20% in females but not males. Following CIS, the density of MORs increases in the cytoplasm of small and large PARV labeled dendrites in females. Moreover, the proportion of near-plasmalemmal MORs compared to the total in large PARV-labeled dendrites decreases in females. After CIS, no changes in the density or trafficking of MORs are seen in the PARV-labeled dendrites in males.